PHYSICAL REVIEW LETTERS

Noise Correlations in Three-Terminal Diffusive Superconductor–Normal-Metal–Superconductor Nanostructures

B. Kaviraj,[1] O. Coupiac,[1] H. Courtois,[2] and F. Lefloch[1,*]

[1]*SPSMS/LaTEQS, UMR-E 9001, CEA-INAC and Université Joseph Fourier, Grenoble, France*
[2]*Institut Néel, CNRS and Université Joseph Fourier, Grenoble, France*

We present measurements of current noise and cross correlations in three-terminal superconductor–normal-metal–superconductor (S-N-S) nanostructures that are potential solid-state entanglers thanks to Andreev reflections at the N-S interfaces. The noise-correlation measurements spanned from the regime where electron-electron interactions are relevant to the regime of incoherent multiple Andreev reflection. In the latter regime, negative cross correlations are observed in samples with closely spaced junctions.

Nonlocal entanglement—the emblematic ingredient to quantum physics—has been proposed and debated for nearly more than a century [1]. Having already been demonstrated in photons [2], it remains difficult to observe for massive particles like electrons. One interesting approach is to perform noise-correlation measurements using superconductors, as they are natural sources of entangled electrons. In mesoscopic systems, nonequilibrium current noise measurements provide information on the charge and statistics of current-carrying states [3]. For noninteracting electrons, the Pauli exclusion principle dictates the zero-frequency cross correlations to be negative [4], whereas no such rule applies in the presence of interactions. In early experiments on electronic analogues of the Hanbury-Brown–Twiss [5] experiment, noise correlations came out to be negative. For beams of partitioned electrons using high mobility GaAs two-dimensional electron gases (2DEG), anticorrelations were revealed, thus illustrating that fermions exclude each other [6]. Fermionic correlations have also been observed for free electrons [7] and neutrons [8]. Interestingly, positive correlations observed in a purely normal 2DEG were ascribed to different scattering mechanisms within the device [9]. Recently, cross correlations with a bias-dependent sign were reported in a three-terminal superconducting hybrid nanostructure with tunnel contacts [10].

In a superconducting hybrid (N-S) beam splitter made of two normal-metal (N) leads in contact with a superconductor (S), an incident electron (hole) from one lead can be reflected at the superconductor interface as a hole (electron) propagating into the other lead. This nonlocal crossed Andreev reflection (CAR) process corresponds to the transfer (creation) of a superconducting Cooper pair into (from) two entangled electrons in the two leads [11]. It creates positive correlations between currents flowing in each of the two leads [12]. On the contrary, elastic cotunneling of an electron (hole) from one lead to the other contributes to negative correlations [13]. Whereas negative correlations are expected from a semiclassical approach neglecting

proximity effect [14], positive correlations at subgap energies are predicted for intermediate values of transparencies [15]. Positive correlations could also arise from synchronized Andreev reflections [16]. In a normal-metallic dot connected to all superconducting leads, positive or negative correlations are expected, depending upon properties of contacts between the dot and its leads [17].

In a S-N-S junction, charge transfer is mediated by multiple Andreev reflections (MAR), a process during which quasiparticles undergo successive Andreev reflections at both interfaces until their energy reaches the superconducting gap. At a bias above the Thouless energy $E_{\mathrm{Th}} = \hbar D / L^2$, where D is the diffusion constant and L is the junction length, MAR are not phase correlated. In this incoherent MAR (IMAR) regime, the noise has been found to be very much enhanced compared to the normal case due to the confinement of the subgap electrons in the sandwiched normal metal [18]. In the same regime, cross correlations are also predicted to be enhanced due to IMAR processes [17]. At low bias voltage, when the time taken by the quasiparticles to reach the superconducting gap exceeds the electron-electron interaction time, the IMAR cycle is interrupted. In this hot electron regime, a Fermi-Dirac-like distribution with an elevated effective temperature is then restored [18].

In this Letter, we present measurements of noise and cross correlations in three-terminal diffusive S-N-S nanostructures. In the IMAR regime, we demonstrate negative correlations in samples where the two junctions are closely spaced.

Samples comprising three-terminal double S-N-S junctions [see scanning electron micrograph (SEM) pictures in Fig. 1] were fabricated by multiple angle evaporation through a PMMA-PMMA/MAA bilayer mask in an ultrahigh vacuum chamber. Evaporation of Cu with a 50 nm thickness was followed immediately by the evaporation of 500 nm-thick Al electrodes, thereby forming diffusive S-N-S junctions across the Cu bridge with highly transparent S-N interfaces. The width of the Cu part was 0.9 μm.
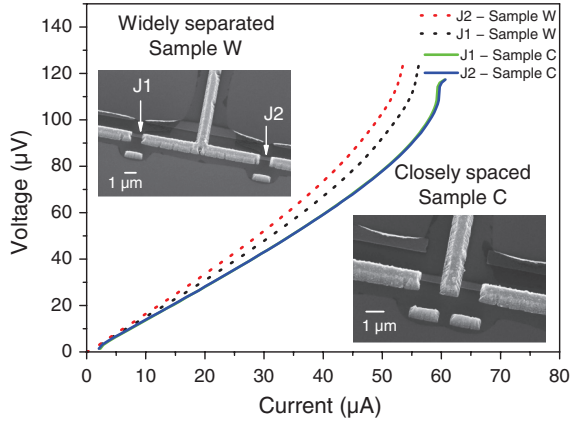
FIG. 1 (color online).   Current-voltage characteristics of each junction J_1 and J_2 of samples W and C at 100 mK. Insets: SEM pictures of both sample geometries. The distance between junctions is 10 μm for sample W and 0.5 μm for sample C.

The samples have two different distances between junctions: 10 μm for the widely separated junctions (sample W) and 0.5 μm for the closely spaced ones (sample C). In the latter case, their distance is comparable with the superconducting Al coherence length, thus making CAR and elastic cotunneling probable. Here, we discuss results obtained on two samples W and C with a junction length $L = 1.3$ μm.

Figure 1 depicts I-V characteristics of individual junctions of the two samples at 100 mK. The junction resistances of a given sample are very much symmetrical, although they differ slightly in the widely separated geometry. All junctions show a superconducting branch with a small critical current (of the order of a few μA), followed by a linear part corresponding to the normal-state resistance of the normal metal, of the order of 1.5Ω. The related Thouless energy is estimated to be about 5 μeV. The abrupt transition in I-V curves at large currents ($\gtrsim 50$ μA) is due to depairing effects in the superconducting Al electrodes. The temperature dependence of the I-V characteristics (not shown) does not show much variation, apart from the depairing current, which decreases at higher temperatures and vanishing critical currents.

We have used a new experimental setup especially designed to measure current fluctuations and noise cross correlations in three-terminal devices at low temperatures. The experiment operates down to 30 mK and is equipped with three commercial SQUIDs (superconducting quantum interference devices) as sensitive current amplifiers, see Fig. 2. Each junction (arm) of the sample is connected to the input coil of a SQUID sitting in the helium bath at 4.2 K. A reference resistor $R_{\rm ref}$ of low resistance (0.092Ω) together with a third SQUID coil is connected in parallel to the sample for voltage biasing. Voltage probes allow us to measure the voltage drop across each junction (V_1, V_2) and across the reference resistor ($V_{\rm ref}$). We found that $V_1 \simeq V_2$
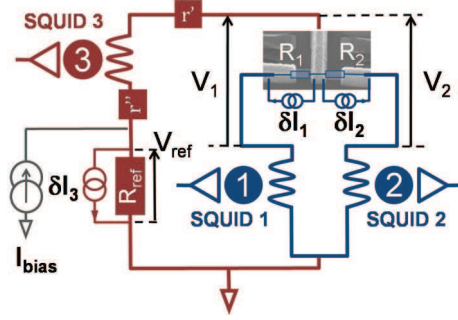

FIG. 2 (color online).   Schematics of the circuit consisting of the sample, each junction being represented by differential resistors R_1 and R_2, and the three SQUIDS to measure the current fluctuations. The reference resistor $R_{\rm ref}$ is used to voltage bias the sample. According to Nyquist representation, each resistance in the model is associated with a current source in parallel. The two additional resistors r' and r'' ($r' + r'' = r$) are due to contact between distinct superconducting elements. Their temperatures are the bath temperature and 4.2 K, respectively. Their associated noise source is not shown for clarity.

but $V_{\rm ref}$ differs slightly from $V_{1(2)}$. This difference, of about 5%, is due to an additional resistor between the sample and the reference resistor. For the two samples discussed here, it corresponds to a resistance $r \simeq 40$ mΩ, which is not negligible compared to $R_{\rm ref}$ and needs to be taken into account in the model discussed below. The intrinsic noise level of each SQUID expressed in equivalent current at its input coil is of a few pA/$\sqrt{\rm Hz}$. At frequencies above a few hundred Hertz, $1/f$ noise contributions were negligible for all bias currents, so that a frequency domain between 0.8 and 4 kHz was chosen for the noise and correlation measurements.

In accordance with Nyquist representation, each resistive part of the circuit is associated with a current source δI_i. The two junctions of a sample are represented as two nonlinear resistors R_1 and R_2. Each SQUID measures partially each of the three current sources [19]. From the three fluctuating SQUID currents $\delta I_{\rm sq}^i$, we can perform three autocorrelations $AC_i \equiv \delta I_{\rm sq}^i \delta I_{\rm sq}^i$ and three cross correlations $XC_{ij} \equiv \delta I_{\rm sq}^i \delta I_{\rm sq}^j$ nonindependent measurements. The spectral densities of noise AC_i and correlations XC_{ij} are related to the physical quantities $S_i \equiv \delta I_i \delta I_i$ and $S_{ij} \equiv \delta I_i \delta I_j$ through a 6 $\times$ 6 matrix. Here, S_1 and S_2 are the noise of each junction of a sample and S_3 the thermal noise of the resistor ($R_{\rm ref} + r$).

Figure 3 shows the six raw datas $\{AC_i\}$ and $\{XC_{ij}\}$ as a function of the voltage drop across sample W. The sum $AC_1 + AC_2 + AC_3 + 2(XC_{12} + XC_{13} + XC_{23})$ is constant thanks to current conservation law, but nonzero due to the noise and correlation backgrounds of the experimental setup. In order to extract the quantities of interest S_1, S_2, and S_{12}, one needs to choose three independent measurements. We chose to focus on AC_1, AC_2, and XC_{12}, which,
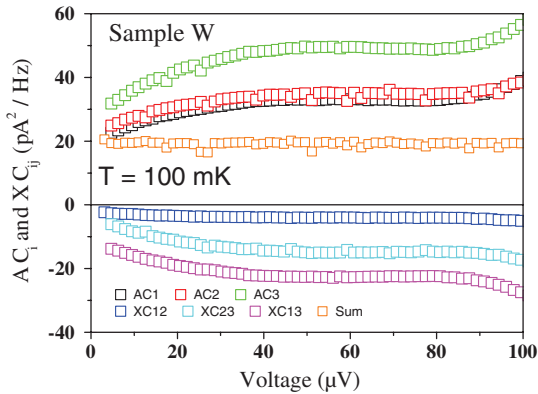
P H Y S I C A L R E V I E W L E T T E R S

FIG. 3 (color online). Raw data of AC_i's and XC_{ij}'s from sample W. The sum represented by the curve along about 20 pA^2/Hz level is constant, as expected, but nonzero due to the setup background noise.

FIG. 4 (color online). Spectral density of noise S_1 and S_2 and cross correlation S_{12} of sample W at 100 mK, obtained using Eq. (1). The lines correspond to the IMAR noise prediction Eq. (2) for each individual junction. The dashed region indicates the interacting hot electron regime, where Eq. (2) is no longer valid.

up to the first order, are close to S_1, S_2, and S_{12}. In a matrix form, the equations of the system reduce to

$$\begin{bmatrix} S_1 \\ S_2 \\ S_{12} \end{bmatrix} = [M^{-1}]\left(\begin{bmatrix} AC_1 - AC_1^0 \\ AC_2 - AC_2^0 \\ XC_{12} - XC_{12}^0 \end{bmatrix} - [N]S_3\right) \quad (1)$$

where AC_1^0, AC_2^0, and XC_{12}^0 represent the background noise and correlation of the setup. Finding S_1, S_2, and S_{12} thus relies on the determination of the noise and correlation backgrounds, as well as of the thermal noise S_3. The elements of the 3×3 matrix $[M^{-1}]$ and of the vector $[N]$ depend only on the differential resistance of each junction and on the resistance $R_{\text{ref}} + r$.

Let us first discuss the case of sample W, where zero correlations ($S_{12} = 0$) are expected. For a S-N-S junction in the IMAR regime, the shot noise in the diffusive case $2eI/3$ is amplified by the number $1 + 2\Delta/eV$ of times a quasiparticle is Andreev reflected before it reaches the gap edge [20]:

$$S(V) = \frac{1}{3}2eI\left[1 + \frac{2\Delta}{eV}\right], \quad (2)$$

where Δ is the superconducting gap. Neglecting the contribution of XC_{12} to $S_{1(2)}$ [19], we adjusted AC_1^0, AC_2^0, and $\Delta = 170 \ \mu$eV so that S_1 and S_2 fit this expression. As inelastic collisions are neglected here, Eq. (2) is valid in a voltage range that is limited but enough to achieve a reliable fit. Knowing AC_1^0 and AC_2^0 and choosing $XC_{12}^0 = 0$ first, we can plot the correlation S_{12}. Our analysis shows that, in order to obtain a bias-independent S_{12}, we need to consider the spurious resistance r as being split into two parts r' and r'' sitting at the mixing chamber with a temperature T and 4.2 K, respectively. The best result is obtained for $r' = 15 \ \text{m}\Omega$ and $r'' = 25 \ \text{m}\Omega$, see Fig. 4.

Finally, by choosing XC_{12}^0, we get S_{12} equal to zero over almost the entire voltage range. It differs from zero only at
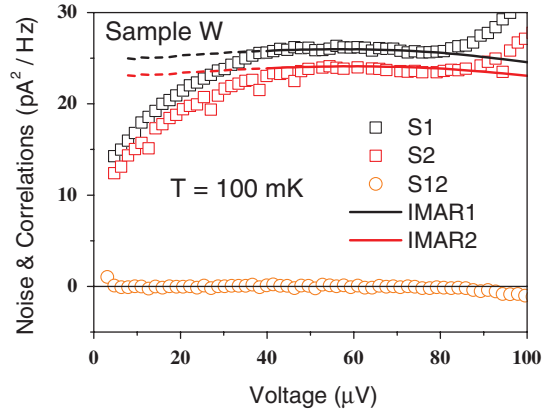
higher voltages approaching the depairing regime, where the common superconducting electrode becomes resistive and the model is no longer valid. From calibration measurements, we know that, due to the current bias, the electronic temperature of R_{ref} can reach up to 300 mK from a bath temperature of 100 mK. However, this has only a minor effect here since most of the noise S_3 comes from the resistance r'' sitting at 4.2 K [19].

For sample C with closely spaced junctions, the measured contact resistance r has the same value as that of sample W. The results can therefore be analyzed exactly the same way as above. In order to adjust the correlation background XC_{12}^0 value, we consider the low bias regime. Here, the noise of each junction is thermal with an elevated effective electron temperature. The two noise sources $\delta I_{1(2)}$ can then be assumed as uncorrelated and hence the cross-correlation noise is zero at low bias: $S_{12}(V \simeq 0) = 0$. We used this criteria to determine XC_{12}^0.

The overall results of noise and correlations for the two different geometries are depicted in Fig. 5 for different temperatures from 100 to 700 mK. Clearly, the two samples show different cross-correlation behaviors above a voltage of about 40 μV, which corresponds to the crossover between the hot electron regime and the IMAR regime. For sample C in the IMAR regime, correlations are negative, up to the depairing regime. When the temperature is increased, thermally activated quasiparticles generate additional thermal noise [18,20]. As these fluctuations are uncorrelated, correlations are expected to exhibit a negligible temperature dependence. This contrast in behavior is actually observed in Fig. 5. In addition to the two samples discussed here, other samples with the same geometry but a different junction length of 1 μm were studied and produced very similar results. For these shorter junctions, the noise level is larger since the resistance is
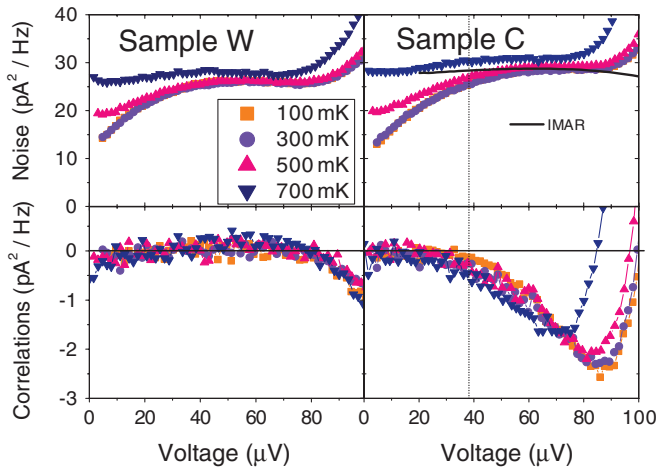
FIG. 5 (color online).   Spectral density of noise S_1 and cross correlation S_{12} of the two samples W and C for various temperatures from 100 to 700 mK. The noise S_2 would give very similar results to that of S_1. The solid line reproduces the IMAR predictions of Eq. (2), whereas the dashed line enlightens that negative correlations appear in the IMAR regime.

lower, see Eq. (2). Again, correlations were found to be zero in the sample with widely separated junctions and negative in that with closely spaced junctions.

Negative correlations are expected for fermionic systems. Therefore, our results suggest that negative correlations arise from partition of quasiparticles injected above the superconducting gap as the result of IMAR processes. When IMAR processes are interrupted by inelastic collisions, the quasiparticle current is reduced and correlations vanish. This is in agreement with our findings. A quasiparticle current is known to vanish over the quasiparticle diffusion length, of the order of a few μm in Al [21]. Zero correlations are thus expected in samples with widely separated junctions, as observed. To our knowledge, the role of the quasiparticle current on correlations has never been investigated theoretically. It may restrict the possibility to observe positive correlations in three terminal devices with all superconducting contacts.

In conclusion, we have measured negative cross correlations in three-terminal diffusive S-N-S nanostructures in the incoherent multiple Andreev reflections regime. This experiment opens the way towards a better understanding of nonlocality and entanglement in superconducting nanodevices with various interface transparencies and bias schemes.

*francois.lefloch@cea.fr
[1] A. Einstein, B. Podolsky, and N. Rosen, Phys. Rev. **47**, 777 (1935).
[2] A. Aspect, P. Grangier, and G. Roger, Phys. Rev. Lett. **47**, 460 (1981).
[3] Y. M. Blanter and M. Büttiker, Phys. Rep. **336**, 1 (2000).
[4] M. Buttiker, Phys. Rev. B **46**, 12 485 (1992); M. Büttiker, Phys. Rev. Lett. **65**, 2901 (1990); M. Büttiker, Physica (Amsterdam) **175B**, 199 (1991); T. Martin and R. Landauer, Phys. Rev. B **45**, 1742 (1992).
[5] R. Hanbury Brown and R. Q. Twiss, Nature (London) **177**, 27 (1956).
[6] W. Oliver, J. Kim, R. C. Liu, and Y. Yamamoto, Science **284**, 299 (1999); M. Henny, S. Oberholzer, C. Strunk, T. Heinzel, K. Ensslin, M. Holland, and C. Schöenenberger, Science **284**, 296 (1999).
[7] H. Keisel, A. Renz, and F. Hasselbach, Nature (London) **418**, 392 (2002).
[8] M. Iannuzzi, A. Orecchini, F. Sacchetti, P. Facchi, and S. Pascazio, Phys. Rev. Lett. **96**, 080402 (2006).
[9] S. Oberholzer, E. Bieri, C. Schönenberger, M. Giovannini, and J. Faist, Phys. Rev. Lett. **96**, 046804 (2006).
[10] J. Wei and V. Chandrasekhar, Nature Phys. **6**, 494 (2010).
[11] J. M. Byers and M. E. Flatté, Phys. Rev. Lett. **74**, 306 (1995); G. Deutscher and D. Feinberg, Appl. Phys. Lett. **76**, 487 (2000).
[12] J. Börlin, W. Belzig, and C. Bruder, Phys. Rev. Lett. **88**, 197001 (2002); P. Samuelsson and M. Büttiker, ibid. **89**, 046601 (2002); P. Recher, E. V. Sukhorukov, and D. Loss, Phys. Rev. B **63**, 165314 (2001).
[13] G. Bignon, M. Houzet, F. Pistolesi, and F. W. J. Hekking, Europhys. Lett. **67**, 110 (2004).
[14] K. E. Nagaev and M. Büttiker, Phys. Rev. B **63**, 081301 (2001).
[15] J. Torrès and Th. Martin, Eur. Phys. J. B **12**, 319 (1999); J. Torrès, Th. Martin, and G. B. Lesovik, Phys. Rev. B **63**, 134517 (2001).
[16] R. Mélin, C. Benjamin, and T. Martin, Phys. Rev. B **77**, 094512 (2008); A. Freyn, M. Flöser, and R. Mélin, Phys. Rev. B **82**, 014510 (2010).
[17] S. Duhot, F. Lefloch, and M. Houzet, Phys. Rev. Lett. **102**, 086804 (2009).
[18] C. Hoffmann, F. Lefloch, M. Sanquer, and B. Pannetier, Phys. Rev. B **70**, 180503(R) (2004); E. Lhotel, O. Coupiac, F. Lefloch, H. Courtois, and M. Sanquer, Phys. Rev. Lett. **99**, 117002 (2007).
[19] See Supplemental Material at http://link.aps.org/supplemental/10.1103/PhysRevLett.107.077005 for the expressions of different SQUID currents and the effect of the temperature of the spurious resistor r.
[20] E. V. Bezuglyi, E. N. Bratus', V. S. Shumeiko, and G. Wendin, Phys. Rev. Lett. **83**, 2050 (1999); K. E. Nagaev, Phys. Rev. Lett. **86**, 3112 (2001).
[21] F. Hübler, J. Camirand Lemyre, D. Beckmann, and H. v. Löhneysen, Phys. Rev. B **81**, 184524 (2010).

SQUID currents equations.

In accordance with Nyquist representation, each resistive part of the circuit is associated with a current source δI_i with $i = 1, 2$ or 3. The two junctions of a sample are represented as two non-linear resistors R_1 and R_2, see Fig. 2 of the main text. The current fluctuations through each SQUID can thus be expressed as:

$$\delta I_{sq}^i = \left(\frac{R_i}{R_i + R_{jk}}\right) \delta I_i - \left(\frac{R_{jk}}{R_i + R_{jk}}\right) (\delta I_j + \delta I_k) \quad (1)$$

where i, j and $k \in \{1, 2, 3\}$ and R_{jk} is the equivalent resistance of R_j in parallel to R_k. The third resistor R_3 in the model correspond to $R_{ref} + r$. From the three fluctuating SQUID currents δI_{sq}^i, we can perform three auto-correlations $AC_i \equiv \delta I_{sq}^i \delta I_{sq}^i$ and three cross-correlations $XC_{ij} \equiv \delta I_{sq}^i \delta I_{sq}^j$ non-independent measurements given by:

$$\begin{aligned} AC_i &= < FFT^*(\delta I_{sq}^i) FFT(\delta I_{sq}^i) > \\ XC_{ij} &= < FFT^*(\delta I_{sq}^i) FFT(\delta I_{sq}^j) > \end{aligned} \quad (2)$$

where FFT stands for the $Fast Fourier Transform$, FFT^* its complex conjugate and $< ... >$ the rms average at the spectrum analyzer.

The spectral densities of noise $\{AC_i\}$ and cross-correlations $\{XC_{ij}\}$ are related to the physical quantities $S_i \equiv \delta I_i \delta I_i$ and $S_{ij} \equiv \delta I_i \delta I_j$ through a 6 x 6 matrix:

$$\begin{bmatrix} AC_1 \\ AC_2 \\ AC_3 \\ XC_{12} \\ XC_{23} \\ XC_{13} \end{bmatrix} = [M_{6 \times 6}] \begin{bmatrix} S_1 \\ S_2 \\ S_3 \\ S_{12} \\ S_{23} \\ S_{13} \end{bmatrix} \quad (3)$$

However, since R_{ref} and r are macroscopic resistors sitting far apart from the sample, we consider that $S_{13} = S_{23} = 0$. The SQUID current equations reduce then to a 6x4 matrix. As an example, the 6x4 matrix for $R_1 = R_2 = 1.5\Omega$ and $R_3 = R_{ref} + r = 0.1\Omega$ is :

$$[M_{6 \times 4}] = \begin{bmatrix} 0.885813 & 0.00346021 & 0.00346021 & -0.110727 \\ 0.00346021 & 0.885813 & 0.00346021 & -0.110727 \\ 0.778547 & 0.778547 & 0.0138408 & 1.55709 \\ -0.0553633 & -0.0553633 & 0.00346021 & 0.889273 \\ 0.0519031 & -0.83045 & -0.00692042 & -0.778547 \\ -0.83045 & 0.0519031 & -0.00692042 & -0.778547 \end{bmatrix} \quad (4)$$

As the six equations relating the six possible measurements, $\{AC_i\}$ and $\{XC_{ij}\}$, to the four quantities, $\{S_i\}$ and S_{12}, are not independent, the set of equations needs to be reduced to three independent equations. For this,

we assume that the spectral density of noise S_3 generated by the resistance $R_3 = R_{ref} + r$ is only thermal. The SQUID equations reduce then to :

$$\begin{bmatrix} AC_1 \\ AC_2 \\ XC_{12} \end{bmatrix} = [M] \begin{bmatrix} S_1 \\ S_2 \\ S_{12} \end{bmatrix} + [N] S_3 + \begin{bmatrix} AC_1^0 \\ AC_2^0 \\ XC_{12}^0 \end{bmatrix} \quad (5)$$

where we have introduced the noise and correlation backgrounds AC_1^0, AC_2^0 and XC_{12}^0 of SQUIDS 1 and 2. The matrix $[M]$ is now a 3x3 matrix and $[N]$ a vector, whose elements depend only on the differential resistance of each junction and on the resistance $R_{ref} + r$.

To obtain the noise spectral densities S_1 and S_2 and the correlations S_{12} we need to inverse the new 3x3 matrix. We then obtain :

$$\begin{bmatrix} S_1 \\ S_2 \\ S_{12} \end{bmatrix} = [M^{-1}] \left(\begin{bmatrix} AC_1 - AC_1^0 \\ AC_2 - AC_2^0 \\ XC_{12} - XC_{12}^0 \end{bmatrix} - [N] S_3 \right) \quad (6)$$

Again, as an example, the inverse matrix $[M]^{-1}$ for $R_1 = R_2 = 1.5\Omega$ and $R_3 = R_{ref} + r = 0.1\Omega$ reads :

$$[M^{-1}] = \begin{bmatrix} 1.13778 & 0.00444444 & 0.142222 \\ 0.00444444 & 1.13778 & 0.142222 \\ 0.0711111 & 0.0711111 & 1.14222 \end{bmatrix} \quad (7)$$

Effect of the temperature of the spurious resistor r

As the additional resistor r is due to contact between distinct superconducting wiring elements, it can be split into two parts r' and r'' sitting at the mixing chamber with a temperature T and 4.2 K respectively. The noise power S_3 is then

$$S_3 = 4k_B[(R_{ref} + r')T + r'' \times 4.2]/(R_{ref} + r)^2 \quad (8)$$

To analyze the noise and correlations results of sample W, we proceed in two steps. As a first step, we only consider S_1 and S_2 and suppose that R_{ref} and r are at the bath temperature T (r' $= 40m\Omega$ and r'' $= 0$ in Eq 8). We adjust AC_1^0, AC_2^0 and $\Delta = 170\mu eV$ so that S_1 and S_2 fit the IMAR prediction (Eq. 2 of the main text), see Fig. 4 of the main text. Here, we neglect the contribution of XC_{12} to $S_{1(2)}$, which is supported by the facts that XC_{12} is much smaller than $AC_{1(2)}$ and that the matrix elements coupling XC_{12} to $S_{1(2)}$ are small numbers.

Once we have estimated AC_1^0, AC_2^0, we can plot S_{12} using equation 6 and choosing $XC_{12}^0 = 0$ first. At this stage, we see in Fig. 1 of this Supplemental Material,
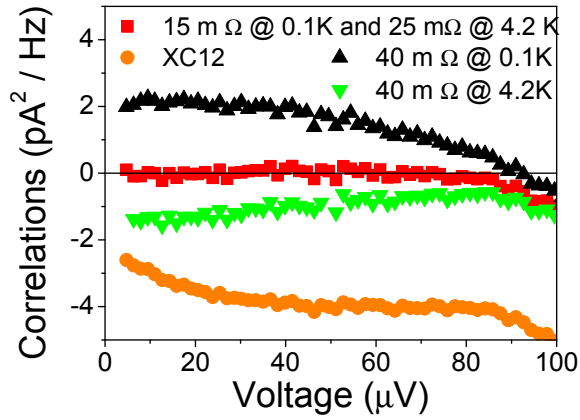
FIG. 1. Cross-correlation S_{12} between the two junctions of the sample W at 100 mK for various choices of the additional contact resistance split between the mixing chamber and the 4.2 K stages on the correlation amplitude S_{12}.

that the noise correlations S_{12} is not constant as a function of the voltage (up triangle black symbols). We can also consider that the resistor r is entirely due to contact at the SQUID having therefore a temperature of 4.2K ($r' = 0$ and $r'' = 40m\Omega$ in Eq 8). Again the S_{12} is not constant (down triangle green symbols). We then adjust r' and r'' so that the noise correlations S_{12} becomes bias-independent. The new expression for S_3 is then fed back in Eq. 6 for iterative and fine adjustment of the parameters values. The best result is obtained for $r' = 15$ mΩ and $r'' = 25$ mΩ. Finally, XC_{12}^0 is adjusted to get S_{12} equal to zero almost over the entire voltage range (square red symbols). Since the contact resistance is found to be the same for sample C, we use the same split of the additional resistor r to analyze the data obtained on that sample with closely-spaced junctions.